Vibration Stimulation as a Non-Invasive Approach to Monitor the Severity of Meniscus Tears

Mohsen Safaei, Nicholas B. Bolus, Daniel C. Whittingslow, Hyeon-Ki Jeong, Alper Erturk, and Omer T. Inan, *Senior Member, IEEE*

Abstract—Musculoskeletal disorders and injuries are one of the most prevalent medical conditions across age groups. Due to a high load-bearing function, the knee is particularly susceptible to injuries such as meniscus tears. Imaging techniques are commonly used to assess meniscus injuries, though this approach suffers from limitations including high cost, need for skilled personnel, and confinement to laboratory or clinical settings. Vibration-based structural monitoring methods in the form of acoustic emission analysis and vibration stimulation have the potential to address the limits associated with current diagnostic technologies. In this study, an active vibration measurement technique is employed to investigate the presence and severity of meniscus tear in cadaver limbs. In a highly controlled *ex vivo* experimental design, a series of cadaver knees (n =6) were evaluated under an external vibration, and the frequency response of the joint was analyzed to differentiate the intact and affected samples. Four stages of knee integrity were considered: baseline, sham surgery, meniscus tear, and meniscectomy. Analyzing the frequency response of injured legs showed significant changes compared to the baseline and sham stages at selected frequency bandwidths. Furthermore, a qualitative analytical model of the knee was developed based on the Euler-Bernoulli beam theory representing the meniscus tear as a change in the local stiffness of the system. Similar trends in frequency response modulation were observed in the experimental results and analytical model. These findings serve as a foundation for further development of wearable devices for detection and grading of meniscus tear and for improving our understanding of the physiological effects of injuries on the vibration characteristics of the knee. Such systems can also aid in quantifying rehabilitation progress following reconstructive surgery and / or during physical therapy.

Index Terms—Biomedical sensing, vibroacoustic characterization, knee joint health, knee injury diagnostics, meniscus injury, vibration testing.

Mohsen Safaei, Nicholas B. Bolus, and Hyeon-Ki Jeong are with the School of Electrical and Computer Engineering, Georgia Institute of Technology, Atlanta, GA 30308 USA (e-mail: msafaei@gatech.edu).

Daniel C. Whittingslow is with the School of Medicine, Emory University, Atlanta, GA 30322 USA.

Alper Erturk is with The George W. Woodruff School of Mechanical Engineering, Georgia Institute of Technology, Atlanta, GA 30332 USA.

Omer T. Inan is with the School of Electrical and Computer Engineering, Georgia Institute of Technology, Atlanta, GA 30308 USA, and also with The Wallace H. Coulter Department of Biomedical Engineering, Georgia Institute of Technology, Atlanta, GA 30332 USA.

I. Introduction

THE role of the knee in dynamic load-bearing during daily activities is accompanied by high risk and incidence of acute injury. The meniscus is a piece of cartilage within the knee that absorbs and distributes vertical loading forces and promotes stability, necessary tasks for maintaining natural joint biomechanics [1]. Due to its exposure to high stresses during rotation and twisting motions, the tearing—whether partial or full—of the meniscus is one of the most common knee injuries: meniscal injuries are responsible for around 700,000 partial meniscectomies every year in the United States [2]. While meniscus tears are common among athletes, they are also quite prevalent in older adults and sedentary populations [3].

The diagnosis of meniscus tears is currently performed most commonly and accurately with magnetic resonance imaging (MRI) [4], [5]. However, MRI is an expensive and time-consuming procedure which requires bulky equipment, laboratory settings, and skilled personnel. In addition, the accuracy of MRI in postoperative assessment of the joint during rehabilitation is still limited for the orthopedic community, and in many cases may not be feasible [6], [7]. Often, clinicians rely upon the self-reported symptoms, history of mechanical symptoms, and physical examination to identify the patients with symptoms that can be attributed to meniscal tear, which involves a high level of uncertainty [8]. Performing arthroscopic surgery in the early stages of acute injuries is also widely suggested as a minimally invasive method to avoid degenerative changes in the knee as a result of the pathology, however this technique is still considered a surgical procedure and thus a non-invasive alternative would be preferred [9].

As an alternative technique, investigation of the vibrations associated with joint articulation ("joint sounds," or acoustic emissions of the joint) as an index of joint structure and health has been explored by various researchers [10], [11]. Joint sound analysis provides a non-invasive diagnostic method

that can be deployed at the point-of-care with wearable form factors for ubiquitous use, such as at home [12]. Recent studies have revealed that, by studying characteristics of the acoustic emissions of the knee, injured knees can be distinguished from healthy ones in both *ex vivo* and *in vivo* studies [13], [14]. Despite the promising potential of joint sound analysis in diagnosing knee disorders, the current state of the art is unable to provide information regarding the severity of injuries and incremental recovery of the joint [15].

Stimulating the knee using an external vibration source and measuring the response can be a tool to address the limitations of current vibration-based knee health monitoring systems. The study of vibration transmission through the human body and correlations between the vibroacoustic properties and the structural integrity of soft tissues have been conducted using various vibration-based techniques such as modal analysis and wave-based methods [16], [17]. Modal analysis usually concerns low frequency vibrations (below 20 kHz) and investigates the structural behavior in terms of natural frequencies, mode shapes, and damping characteristics [18]. In contrast, wave-based methods such as guided wave structural health monitoring and elastography often analyze the structural properties at ultrasonic frequencies (from 20 kHz to MHz) [19], [20].

While very few studies have explored the use of modal vibration analysis techniques to diagnose knee injuries such as meniscal tears, there is a long history of using such methods for health monitoring in various natural and prosthetic joints and anatomical compounds. The diagnostic applications of external vibration stimulation were introduced in the early 20th century when the vibration response of the femur, humerus, and clavicle to finger percussion was used to differentiate fractured bones from intact ones [21]. Vibration measurement is a widely proposed method to diagnose bone fracture and to monitor the fixation and healing process [22], [23]. Reduction in the shock absorption capacity of the knee as a result of meniscus tear and meniscectomy is also investigated as a non-invasive measure of the joint health [24]. Another application proposed for the vibration measurement is the osseointegration assessment of medical implants such as dental implants [25]–[27], cementless hip implants [28], [29], and cemented total knee replacements [30], [31] during and after surgery.

The ability of active vibration measurement techniques to track the changes in the structural integrity of physiological tissues can be expanded to the analysis of the severity of the problem using the structural health monitoring (SHM) techniques often employed in mechanical structures. Vibration-based SHM is used for damage detection in various structures with an emphasis on stiffness reduction in the structure as a result of damage, which leads to changes in dynamic characteristics such as natural frequencies, damping ratios, and mode shapes [32]. In particular, frequency-based experimental SHM methods, when coupled with an analytical vibration model of the structure, can reveal information regarding damage status with a single sensor arrangement by comparing the input-output frequency response function (FRF) and the location of natural frequencies [33], [34]. As a common approach in the literature, various structures have been simplified and modeled as a beam with specific boundary conditions representing the interactions between the structure of interest and other components of the system [35]. Often, a crack is modeled as a local elastic component such as a lumped spring to represent changes in the flexural or longitudinal stiffness of the beam. Several studies have modeled beam cracks as massless torsional springs with a stiffness proportional to the severity of the defect [36]–[38]. A similar approach was employed in the present work to investigate the meniscal damage in cadaveric knee joints.

In this study, a vibration-based frequency spectrum analysis was performed on the human knee to investigate the ability of such a technique to detect the occurrence and severity of meniscus injury in cadaveric knee joints. A surgical procedure was devised to simulate meniscus injuries at different stages. External mechanical vibration was used to obtain vibration transmissibility of the joint at each stage, and the resulting FRFs were used to identify the injury. Finally, a beam model of the knee joint was created, and a qualitative and comparative analysis of the effects of the injury on the vibration response of the knee was conducted. This analytical model of the knee was introduced to establish a fundamental qualitative framework capable of simulating the vibroacoustic behavior of the joint, which can be extended to various active and passive vibration-based analyses of the joint structure and its sensitivity to injuries as a local change in the vibration characteristics (e.g. stiffness change).

II. METHODOLOGY

A. Specimen Preparation

Six fresh, frozen human cadaver knees obtained from Med-Cure, Inc. (Orlando, FL) were used in this study. The legs had an average age of 63.6 ± 9.5 years of age. Prior to experiments, the legs were stored at -20 °C and thawed in a water bath at room temperature for 10 hours. The legs did not have any history of major knee disorders, including injuries, arthritis, or surgery. While the age range of the cadavers does not fully represent the overall population of people with knee injuries, these exclusion criteria may mitigate some of the effects on joint structure typically associated with advanced age groups. Manual, repeated flexion-extension of each cadaver limb was conducted prior to data collection to ensure that joints were fully thawed and consistently pre-conditioned (i.e., no residual internal constraints due to shipping and storage at low temperature). The manual flexion-extensions were performed for the full angular range of motion allowed by the leg without excessive force and for a minimum of 10 cycles until an unconstrained motion was achieved based on the examiner tactile feedback. The use of fresh frozen limbs—also employed in training procedures for orthopedic surgeons—ensures that the mechanical properties of the soft tissue and bone are as similar as possible to the *in vivo* case.

B. Meniscus Tear Simulation in Cadaver Legs

Four stages of testing were considered in this study to simulate the effects of meniscus injury, including baseline, sham surgery, meniscus tear, and meniscectomy (Fig. 1).
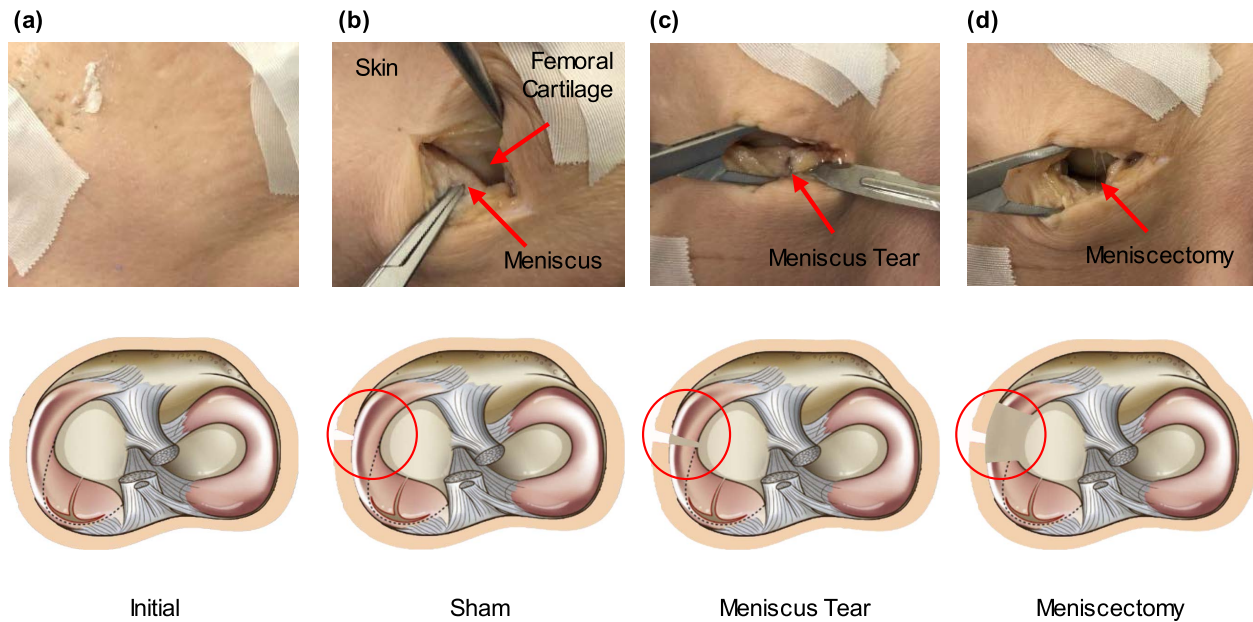
Fig. 1. Injury simulation steps on the cadaver leg including (a) baseline (initial), (b) sham surgery, (c) meniscus tear, and (d) meniscectomy.
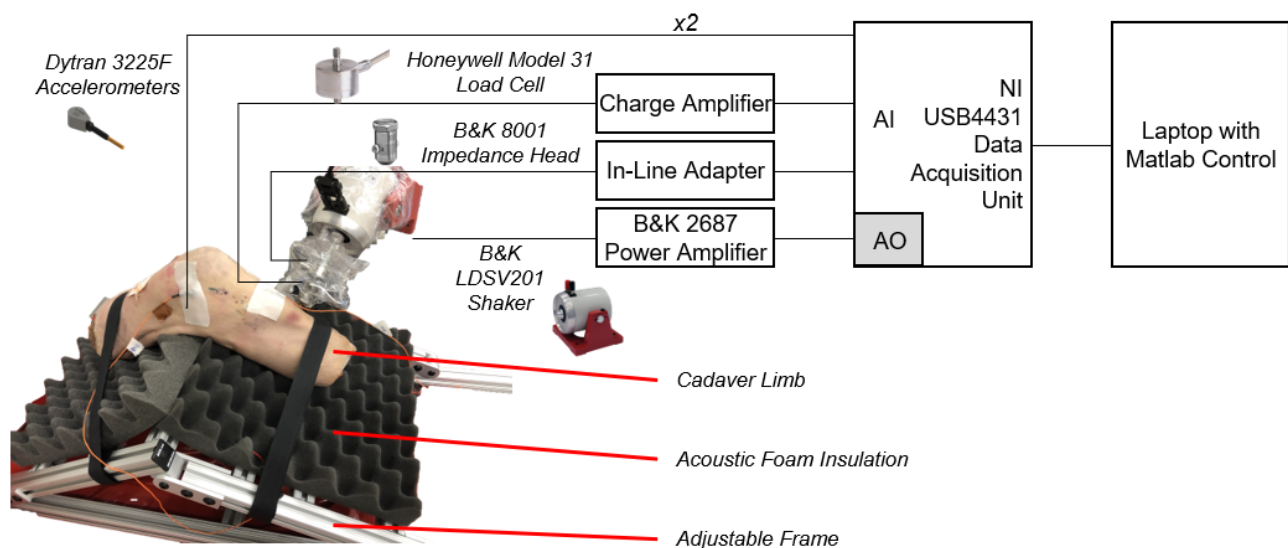

Fig. 2. Knee vibration stimulation setup—including an electrodynamic shaker, a load cell and an impedance head transducer to measure the input, and two accelerometers to measure the response—attached to a cadaver leg positioned on an adjustable frame.

Initial measurements were conducted on the thawed and pre-conditioned knees, and the data were used as the baseline (Fig. 1(a)). The sham surgery included a 4-cm skin incision anterior to the superficial medial collateral ligament (MCL) in parallel with the joint line (approximately on the tibial plateau) onto the knee capsule (Fig. 1(b)). After creating this incision, the medial meniscus was exposed and ready to be surgically altered in the next stage [14]. Extra caution was taken to ensure that the meniscus was intact, and the incisions were closed with continuous sutures prior to vibration testing. Next, to simulate a radial meniscus tear, the sutures binding the skin incision were cut to access the meniscus, and the meniscus was cut with a scalpel radially on the medial aspect (Fig. 1(c)). The access cut through the skin was again sutured identically to the sham stage before vibration measurements were conducted on the altered knee. Finally, the meniscus was

re-exposed by cutting the sutures, and a meniscectomy was performed. At this stage, a 5-mm wide radial section of the meniscus anterior to the simulated tear was surgically removed (Fig. 1(d)), and the incisions were sutured as before prior to collecting the final measurements.

C. Vibration Test Setup

Vibration tests were conducted by placing the cadaver legs on a customized adjustable stand to hold the knees at 45° of flexion, as shown in Fig.2. The sample was fixed on the stand using two Velcro straps and two pieces of acoustic foam insulations to minimize the environment noise transferred through the support. A permanent magnet shaker (LDS V201, Brüel & Kjær, Nærum, Denmark) was used to excite the leg at a location on tibia distal to the joint center medial to the tibial tuberosity. An impedance head transducer (Type 8001,

Brüel & Kjær, Nærum, Denmark) along with a load cell (Model 31, Honeywell International Inc., Charlotte, NC) were attached to the shaker head to record the stimulating vibration amplitude and the static and dynamic forces. The shaker tip was pressed against the skin with an initial force level of 5 N to ensure that the shaker and sample stay in consistent contact throughout the tests. The compression force was selected based on an initial investigation of the comfortable threshold for the live subjects as reported in literature [52], and the maximum amplitude of the dynamic force exerted by the shaker during measurements. Two miniature, high sensitivity, and low mass accelerometers (Type 3225F, Dytran Instruments Inc., Chatsworth, CA) were placed on the medial and lateral aspects of the joint superior to the knee center. The accelerometers were fixed by a thin double-sided tape as well as a flexible backing tape to provide some level of pressure on the back of the sensor and to ensure better contact between the sensor and skin.

The shaker, load cell, impedance head sensor, and accelerometers were connected to a five-channel (four input and one output) data acquisition device (USB 4431, National Instruments, Austin, TX) with IEPE-enabled input ports for the two Dytran accelerometers. The measurements were controlled using a customized MATLAB program (Mathworks, Natick, MA), and the data was sampled at 50 kHz. A swept-frequency cosine excitation signal was fed into the shaker through a power amplifier (Type 2687, Brüel & Kjær, Nærum, Denmark) with a frequency band between 100 Hz and 4200 Hz and a total duration of 180 sec. Since the shaker's response to a fixed input voltage changes over its operating bandwidth, the amplitude of the excitation signal was initially adjusted using single frequency sine signals at frequency intervals of 200 Hz to achieve a constant level of input acceleration throughout the measurement. A sufficiently high and uniform acceleration level was applied, which was high enough to avoid noise over the frequency range of interest but low enough not to trigger any potential nonlinearities.

D. Signal Processing and Feature Extraction

The measured acceleration signals were initially filtered using a Kaiser window finite impulse response bandpass filter with frequency bandwidth between 100 Hz and 4200 Hz to remove the unwanted frequency content (noise). Next, the input-output FRF of the accelerometers were calculated at 8192 frequency points using the transfer function estimator H_1 [18]. The input-output coherence of the measured response was also calculated as a measure of the quality of the measurements. Note that the random noise in the output acceleration can be minimized using the estimator H_1 due to the averaging in the cross power spectral density [39]. To investigate the differences between the FRF results obtained at different stages of the knee injury, the root-mean-square-deviation (RMSD) of FRF (in dB) with respect to the baseline was calculated using Eq. (1).

$$RMSD = \sqrt{\frac{\sum_{k=1}^{n} [FRF_2(k) - FRF_1(k)]^2}{\sum_{k=1}^{n} FRF_1(k)^2}}, \quad (1)$$

where k represents the frequency point number, and subscripts *1* and *2* are the two stages of the joint condition compared to each other. RMSD is one of the most common metrics used in SHM to assess the presence and propagation of damage within the structure [40]. To extract the frequency bands containing statistically significant differences between the FRFs, the RMSD values were calculated for various frequency spans around different center frequencies. Center frequency was varied from 110 Hz to 4390 Hz, and frequency margins of a minimum of 10 Hz increasing in 10 Hz increments were investigated. The maximum frequency band was set to the maximum distance between the center frequency and the lower or higher limits of the entire measurement frequency band (100 Hz and 4200 Hz, respectively). The resultant RMSD matrix was then analyzed using a two-sample Student's t-test to find the frequency bands which represent a significant change in the FRF state of injured legs compared to the sham surgery stage. The normality of the data was confirmed using Kolmogorov-Smirnov test prior to the t-test [41]. Amongst frequency bands with statistical significance, the effect size was calculated using Cohen's d to identify areas with large effects [42]. The RMSD values of the selected frequency bands were considered as the feature representing the occurrence and severity of the meniscus injury. The inter-stage variations were also investigated by calculating the RMSD value of each surgery stage for each subject and comparing these to the average values of the same stage across subjects. Additionally, a multiple comparison test (Fisher's least significant difference) was utilized to compare the changes that occurred at different stages of the knee surgical intervention for the selected features [43]. The signal processing process described herein is demonstrated in Fig. 3.

E. Analytical Model of the Knee Joint With Meniscus Tear

The vibratory behavior of many engineering structures and the change in the vibration transmission as a result of structural damage are often modeled analytically for a fundamental understanding. However, analytical models are limited to relatively simple components, and most complex geometries are usually modeled using numerical methods such as finite element analysis. One solution to the complexity problem is to simplify the geometries and boundary conditions of multifaceted structures into equivalent, conventional mechanical components which can represent targeted physics of the problem in an analytically accessible framework. The knee, with its complicated geometries and intricate, irregular interfaces, is surely a complex structure. Although dynamic models of the knee have been developed for biomechanical analysis of human movement, these models often consider the rigid body dynamics of human body parts and their interactions and are not able to predict the vibroacoustic characteristics of the knee [44]. In this section, a simplified model of the knee joint capable of capturing the qualitative aspects of joint health (meniscus injury) is introduced. The knee is considered as a double beam system with an internal hinge-type joint. A schematic of the beam model is shown in Fig. 4. Two Euler-Bernoulli beams with a translational spring
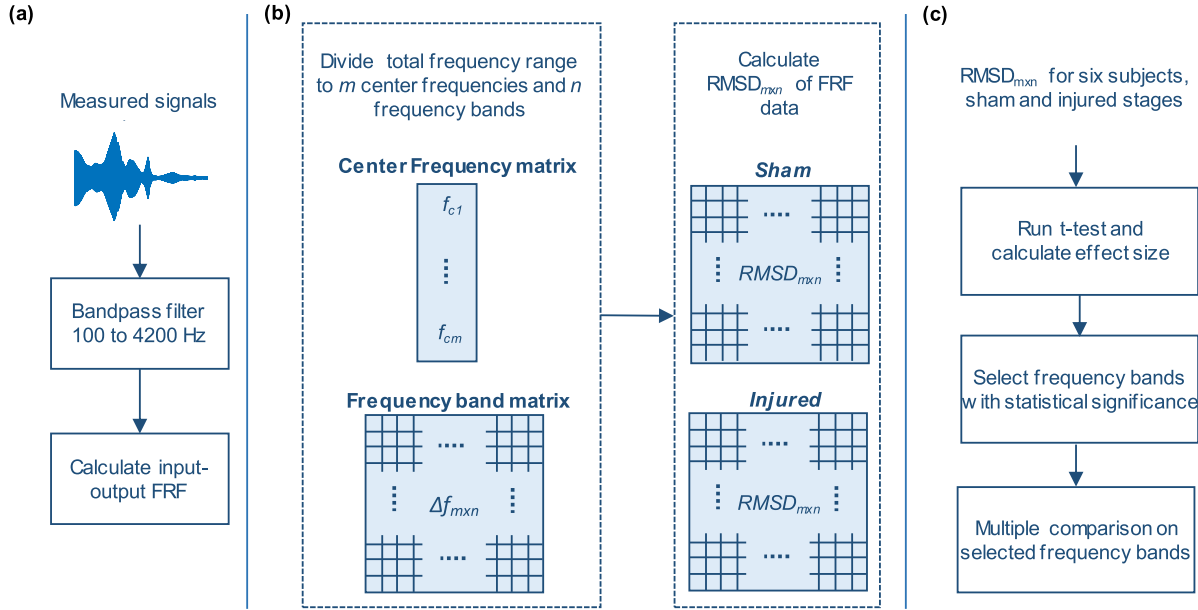
Fig. 3. Signal processing and feature extraction diagram, (a) signal preprocessing using Kaiser window bandpass filter and FRF calculation using H_1 estimator, (b) total frequency band divided to m center frequencies and n frequency bands around the center frequency, RMSD of FRFs for sham and injured with respect to baseline calculated at all bands, and (c) statistical analysis including feature selection and multiple comparison test.
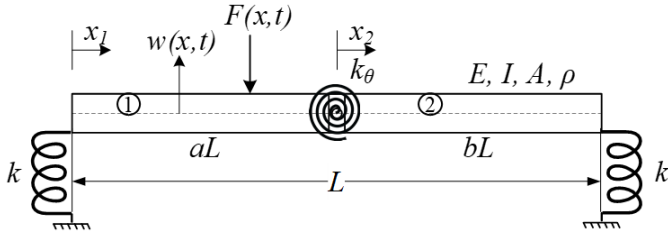

Fig. 4. An equivalent two-segment beam model (to represent tibia and femur) and a torsional spring at the joint (to represent knee injury) in the analytical mode.

(k) at each boundary are connected via a hinged joint equipped with a torsional spring (k_θ). Beams 1 and 2 represent the tibia and femur, respectively, and the torsional spring represents the combined flexion-extension and internal-external rotational stiffness of the joint. The two translational springs simulate the effects of the Velcro straps. As an approximation for qualitative simulations, the flexural rigidity and mass (per length) of the beam segments are assumed to the identical, though it is straightforward to enter separate values in the formulation. Furthermore, shear deformation and rotary inertia effects are neglected (which can be included with a Timoshenko beam type model), and the foam in Fig. 2 is assumed to have negligible stiffness (which can otherwise be accounted for as a Winkler foundation). Briefly the uniform Euler-Bernoulli model is deemed sufficient for a qualitative representation.

It has been demonstrated in the literature that the occurrence of meniscus injury can lead to a reduction in the stiffness of the joint proportional to the severity of the injury [45]. As a result, a change in the torsional stiffness in the current beam model is treated as a representation of meniscus injury and its severity. Equation of motion for the double beam system is given in Eq. (2) [46].

$$EI\frac{d^4 w(x,t)}{dx^4} + c\frac{dw(x,t)}{dt} + \rho A\frac{d^2 w(x,t)}{dt^2} = f(x,t) \quad (2)$$

where $w(x,t)$ is the transverse displacement of the beam, x is the location on the beam, t is time, E is the modulus of elasticity, I is the second moment of area, c is the damping coefficient, ρ is the mass density of the beam per unit of length, A is the cross section of the beam. Furthermore, the external forcing is $f(x,t) = Fe^{j\Omega t}\delta(x - x_F)$, where F is the force amplitude, Ω is the excitation frequency, j is the unit imaginary number, δ is the Dirac delta function, and x_F is the excitation position. Following the standard modal analysis procedure, the vibration response of the two-segment beam can be expressed as:

$$w(x,t) = \sum_{i=1}^{\infty} q_i(t)\phi_i(x) \quad (3)$$

where $q_i(t)$ and $\phi_i(x)$ are the modal coordinates and the mode shapes, respectively.

The solution for the space-dependent part (mode shapes) can be expressed as demonstrated in Eq. (4) for the two beams.

$$\begin{cases} \phi_1(x_1) = & A_1\,\text{Sinh}\,(\lambda x_1) + B_1\,\text{Cosh}\,(\lambda x_1) \\ & +C_1\,\text{Sin}\,(\lambda x_1) + D_1\,\text{Cos}\,(\lambda x_1) \\ \phi_2(x_2) = & A_2\,\text{Sinh}\,(\lambda x_2) + B_2\,\text{Cosh}\,(\lambda x_2) \\ & +C_2\,\text{Sin}\,(\lambda x_2) + D_2\,\text{Cos}\,(\lambda x_2) \end{cases} \quad (4)$$

where subscripts 1 and 2 denote beams 1 and 2, respectively, and $\lambda_i^4 = \frac{\rho A \omega_i^2}{EI}$, where ω_i is the ith natural frequency of the beam. Redefining x coordinate as $x = x/L$ (L is the total length of the beams), eight boundary conditions can be defined for the locations $x_1 = 0$, $x_1 = a$, $x_2 = 0$, and $x_2 = b$.

$$\phi_1''(0) = 0$$
$$\phi_2''(b) = 0$$
$$EI\phi_1''(0) = -k\phi_1(0)$$
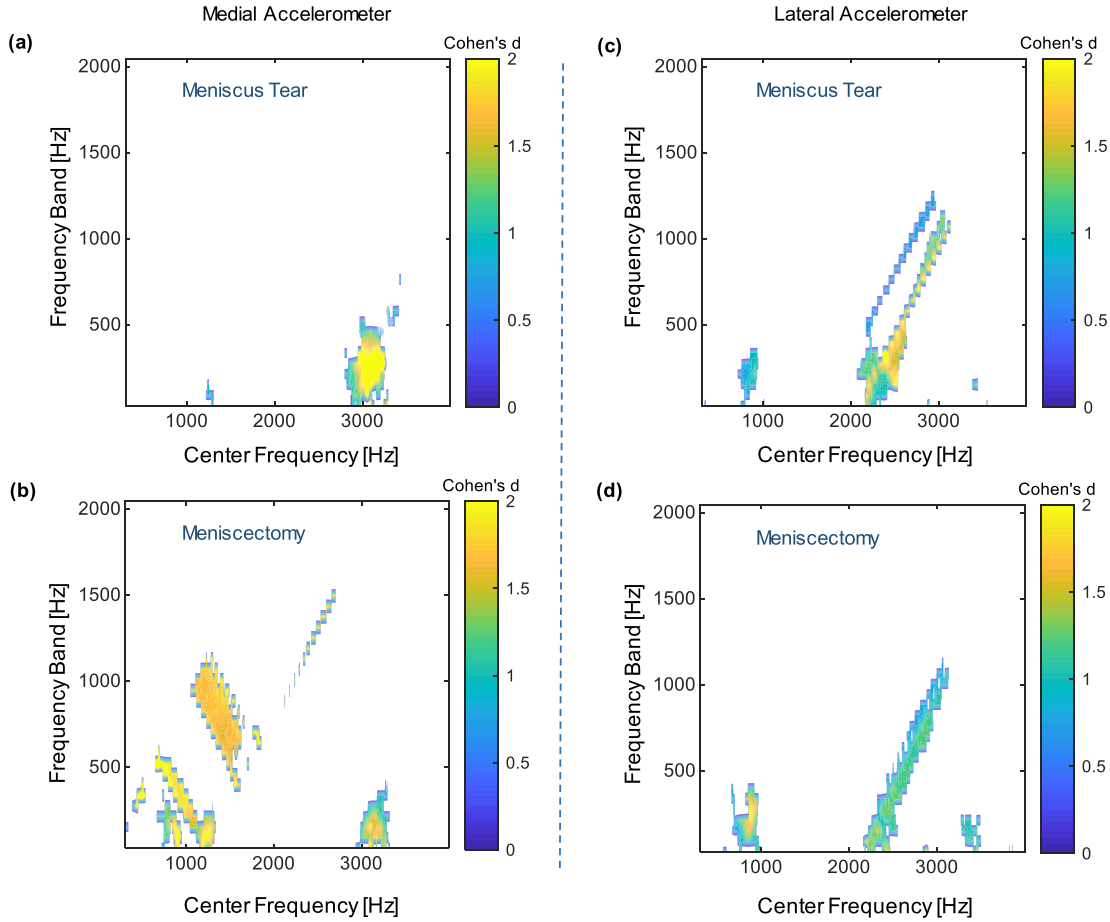$$EI\phi_2''(b) = k\phi_2(b)$$

Fig. 5. Identification of frequency bands (feature extraction) of injured cases with significantly higher RMSD values compared to the baseline for meniscus tear and meniscectomy; (a) and (b) medial accelerometer, (c) and (d) lateral accelerometer, colorbar represents the Cohen's d for the frequency bands.

$$\phi_1(a) = \phi_2(0)$$
$$\phi_1''(a) = \phi_2''(0)$$
$$\phi_1'''(a) = \phi_2'''(0)$$
$$EI\phi_1''(a) = k_\theta\left(\phi_2'(0) - \phi_1'(a)\right). \quad (5)$$

Substituting Eq. (4) in the system of equations in Eq. (5), the characteristic equation and the constants of Eq. (4) can be found. Additionally, the natural frequencies (from eigenvalues) and the mode shapes of the two-segment system can be developed. Substituting Eq. (3) into (2), multiplying by the mode shape, integrating and applying the orthogonality conditions yield

$$\omega_i^2 q_i(t) + 2\xi_i\omega_i\dot{q}_i(t) + \ddot{q}_i(t) = Fe^{j\Omega t}\bar{\phi}_i(x_F), \quad (6)$$

where ξ_i is the modal damping ratio defined as $\xi_i = c/(2\omega_i\rho A)$, and $\bar{\phi}_i$ is the normalized eigenvector given as

$$\bar{\phi}_i(x) = \frac{\phi_i(x)}{\sqrt{\int_0^1 \rho A\phi_i^2(x)}}. \quad (7)$$

Since the system is linear, the particular solution of Eq. (6) is harmonic at the excitation frequency, and it can be expressed as

$$q_i(t) = \frac{F\bar{\phi}_i(x_F)}{\omega_i^2 - \Omega^2 + j2\xi_i\Omega\omega_i}e^{j\Omega t}, \quad (8)$$

TABLE I
DIMENSIONS AND MATERIAL PROPERTIES OF THE KNEE JOINT

Parameter	Value	Parameter	Value
a, b	0.5	Stiffness (k_θ), N.m/rad	100
Diameter (d), mm	45	Young Modulus (E), MPa	20
Stiffness (k), N/m	1	Density, (ρ), kg/m³	1900

where Ω is the frequency of the excitation force. Substituting Eq. (8) in Eq. (3), the steady-state response can be obtained, and the input-output FRF (accelerance) of the beam system can be extracted as

$$\text{FRF} = \sum_{i=1}^{\infty} \frac{-\Omega^2\phi_i(x_m)\bar{\phi}(x_F)}{\omega_i^2 - \Omega^2 + j2\xi_i\Omega\omega_i}. \quad (9)$$

where x_m is the measurement point. Equation (8) is a complex FRF due to the presence of damping, and the magnitude form is of interest in this study. The dimensional parameters and material properties used in the beam model were average values found in the literature for the tibial and femoral bones, as listed in Table I.
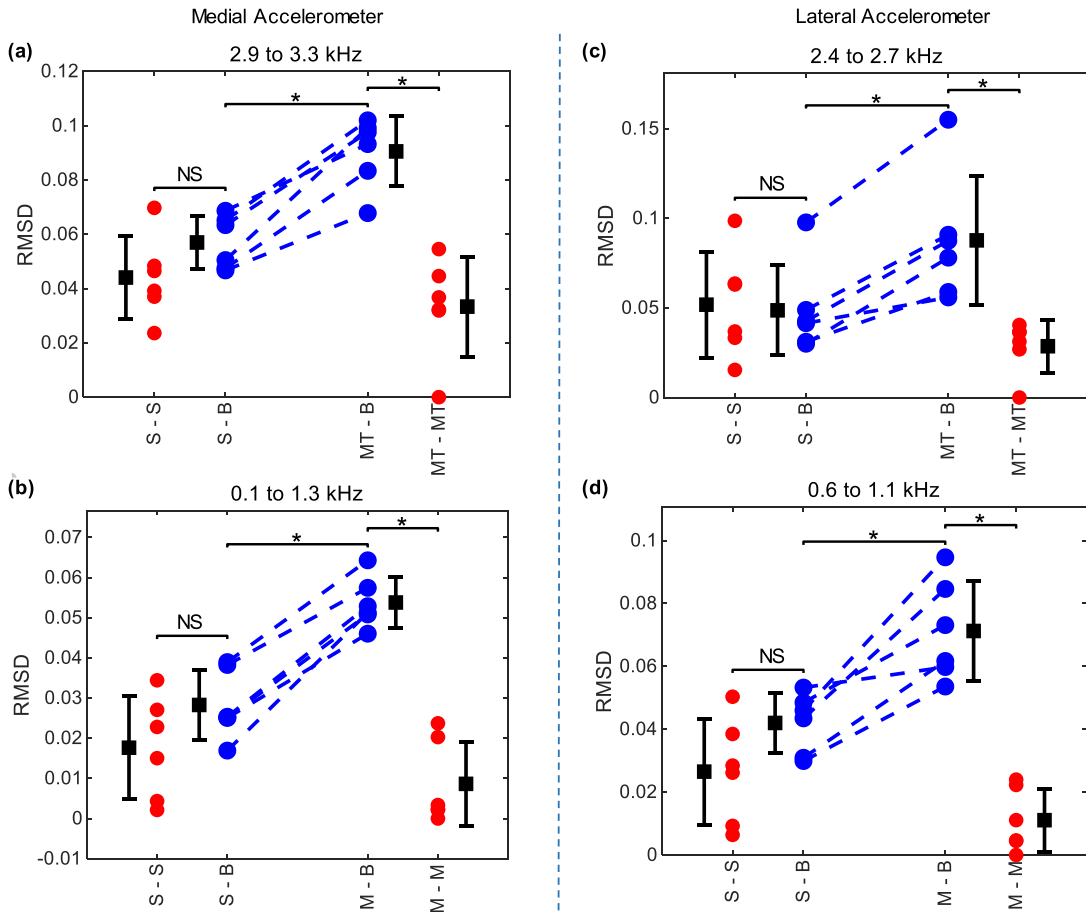
Fig. 6. RMSD values at selected frequency bands in injured cases with a meniscus tear and meniscectomy compared to the sham, and repeatability of sham and injured measurements; (a) and (b) medial accelerometer, (c) and (d) lateral accelerometer. The results present significantly higher RMSD values of the injured cases with respect to the baseline (blue, MT-B and M-B) compared to the sham stage RMSD values (blue, S-B) and intra-stage variations (red). B: baseline, S: Sham, MT: meniscus tear, M: Meniscectomy, *: p < 0.05, NS: not significant.

III. RESULTS AND DISCUSSION

A. Feature Extraction

The RMSD values of meniscus tear and meniscectomy stages with respect to the baseline were calculated for various bandwidths of the signal at the medial and lateral locations and the Cohen's d effect size for the areas with statistically significant differences are plotted in Fig. 5. The occurrence of the meniscus tear can be detected in certain frequency bands at different stages. Both medial and lateral accelerometers are able to detect the tear at a frequency band of about 400 Hz around center frequencies of 3000 Hz and 2500 Hz, respectively. Increasing the severity of the injury by conducting a meniscectomy, the accelerometers are able to detect the changes in the structure using RMSD values at lower frequencies in addition to the higher frequency regions observed in the meniscus tear stage. The meniscectomy is detectable at frequencies around 800 Hz by both medial and lateral accelerometers. The relationship between the detectable size of damage and frequency of propagating elastic waves is a well-known phenomenon in SHM; higher frequency waves can carry information regarding smaller defects due to smaller wavelength [32].

The lower frequency areas are only present in the measurement results from the meniscectomy stage, demonstrating

the potential of vibration measurement in detecting specific type and size of meniscus injury at different frequency bands. Furthermore, larger frequency areas are capable of detecting the injuries on the medial aspect compared to the lateral aspect. Proximity of the medial sensor to the tear location (on the medial meniscus) may also indicate the ability of the vibration technique to identify a localized injury.

As a result of the analysis performed in this section, the RMSD values corresponding to the frequency ranges with the most significant changes are selected as the features of frequency response measurements capable of detecting structural changes in the knee joint associated with meniscus disruption. Frequencies between 2.9 kHz and 3.3 kHz, and 2.4 kHz and 2.7 kHz are chosen for detecting the meniscus tear in medial and lateral accelerometers, respectively. Frequencies between 0.1 kHz and 1.3 kHz, and 0.6 kHz and 1.1 kHz are selected for detecting the meniscectomy at medial and lateral locations, respectively. Selected bands present an effect size of around 2, which shows a large difference between the sham and injury stages [42].

B. Meniscus Tear Monitoring

Using the features extracted in the previous section, the changes in the RMSD values of the measured FRFs are calculated for the tear cases and sham surgery to ensure
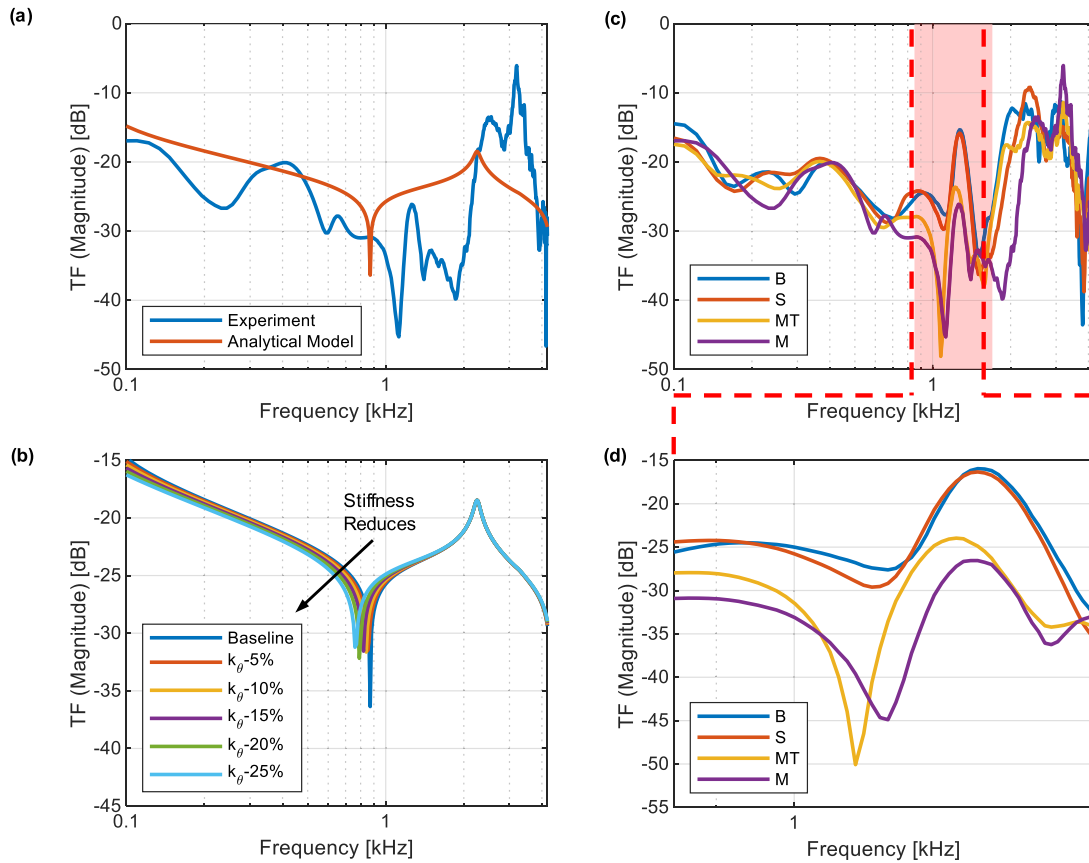
Fig. 7. (a) Comparison of experimental and analytical results, (b) simulated FRFs for various torsional spring stiffnesses, (c) measured FRFs from one of the cadaver legs, and (d) zoomed view of measured FRFs for a frequency range with statistically significant RMSD.

the significance of the results. Fig.6 demonstrates the RMSD values of the selected frequency ranges for all the six specimens with respect to the baseline (blue) at medial and lateral locations. The graphs demonstrate significantly higher RMSD values for the injured cases compared to the sham measurements for all the cases with a p-value of less than 0.05. The changes are consistent for the two tear stages and at the medial and lateral accelerometers

Furthermore, the intra-stage variations in the RMSD values of the sham, meniscus tear, and meniscectomy with respect to the average of the stage are plotted (red). The results present significantly lower values within each stage (red) compared to the RMSD values injured stages with respect to the baseline (blue, MT-B and M-B). Specifically, the variations of FRF data amongst different samples are remarkably lower than the changes in the FRF as a result of the modification of the joint. It also shows that the effects of the experimental setup, such as shaker mounting, sample fixation, and sensor placement, are small. Additionally, the least significant difference test conducted on the results demonstrated that the significant pairwise changes could be observed only between the injured cases and the baseline, again ensuring the significance of the results discussed in this section.

C. Comparison of Model and Experiment

A comparison of the simplified analytical model presented in Sec. II.E and a representative set of data collected experimentally from one of the samples is shown in Fig. 7(a).

While a quantitative prediction and accurate match between the model and experimental results would require extensive measurements of the material properties and dimensions of the knee and a more complicated model of the joint incorporating all the components of the anatomy and their interactions, the simplified beam model is able to demonstrate similar trends as observed in experimental data. Thus, a qualitative assessment of system parameters can be performed using the model to gain a better understanding of the vibration behavior of the joint. To investigate the effects of meniscus injury on the FRF of the knee, the torsional stiffness was decreased in 5% increments. Results are presented in Fig. 7(b) for stiffness changes up to 25% of the initial quantity. The resultant changes in the FRF can be observed mostly around 1 kHz, and the torsional stiffness does not lead to noticeable changes at frequency ranges higher than 1 kHz. Similar behavior has been reported by researchers when studying the ability of vibration-based SHM in detecting defects of various sizes within structures [35], [47].

The experimental FRF diagrams of different stages of the knee for one representative subject is displayed in Fig. 7(c) and (d). The highlighted area in the graph shows a frequency range with significantly higher RMSD values of injured cases compared to the sham case. While the sham surgery results in a slight change in the FRF compared to baseline, meniscus tear, and meniscectomy exhibit a more significant deviation in the measured FRF. Similar to the analytical model, consistent changes in the response can be

observed at specific frequencies. The modal expansion method used in the analytical model solution can explain the variations in the FRF data as a result of the structural alterations. The changes in the meniscus structure due to tear, mostly affect the boundary conditions at the mid-point of the beam by reducing the stiffness (i.e., meniscus tear leads to a reduction in flexion-extension and internal-external rotational stiffness of the joint). The boundaries have a major effect on some modes (in this case, mostly on the fundamental mode) of vibration, while the rest of the modes are more affected by the dimensional parameters and mechanical properties of the beam [48], [49]. Due to the absence of live tissues in the cadaver legs, the effects of meniscal tear on the vibration properties of the knee are local to the boundaries of the beam model. In other words, the injury does not affect the structure of the femur and tibia and only changes the meniscus stiffness represented as a torsional spring in the model. In live subjects, the meniscal injuries also affect the properties of the joint component, including bone, cartilage, joint fluids, meniscus, tendons, ligaments, and other soft tissues surrounding the knee capsule [50], [51]. Therefore, a representative analytical model should incorporate those effects to achieve a comparable analytical and experimental analysis. Moreover, it is worth mentioning that a previous study [52] on the vibration characterization of the human knee joint demonstrated a similar trend in the tibiofemoral vibration transmission of the human knee to the cadaver models, which is promising and partially mitigates concerns around potential translation from cadaver to human use.

IV. CONCLUSION

In this study, experimental and analytical investigations were performed to demonstrate the ability of a vibration-based health monitoring method to detect the occurrence and severity of meniscus injury in the human knee. The study involved vibration stimulation of six cadaver knees and skin-mounted, accelerometer-based measurements of the response of the knee to a continuous frequency sweep cosine excitation. To simulate different grades of a common knee injury (meniscus tear), a surgical procedure was conducted on the legs, and four stages of meniscus integrity were considered; baseline, sham surgery, meniscus tear, and meniscectomy. Furthermore, an analytical model of the joint was created using a two-segment Euler-Bernoulli beam model consisting of two beams connected by a torsional spring in the middle and translational springs on the two ends. The results of experiments showed that the FRF measurements are able to detect the meniscus tear as well as meniscectomy at specific frequency ranges. Using RMSD values of different measurements with respect to the baseline, significant differences (p <0.05) were observed amongst all subjects. Additionally, test and subject variations were included in the analysis, and results showed that significant changes are only present when the joint is surgically altered by a tear.

In an analytical model, the change in joint integrity as a result of meniscus tear was simulated as a reduction in the torsional stiffness of the double beam system. Results demonstrated that noticeable changes in the FRF of the system can be observed at specific frequency ranges. Qualitative results from this model-based simulation analysis were broadly similar to that of experimental testing. While the analytical model was a simplified representation of the knee, the approach and the results thereof enable a better understanding of the vibroacoustic characteristics of the joint as a result of meniscal injury, which can be used in future research to advance the knowledge of the knee vibrations in both active (external stimulation) and passive (acoustic emission) forms.

Overall, results of this work demonstrate the promising potential of external vibration stimulation in diagnosing and grading meniscus injury. However, it is important to note a few limitations to this study. This study was limited to six cadaveric limbs, a sample size that will need to be increased in future work to determine the specific frequency ranges that capture the effects of meniscus damage on the vibration response of the knee more generally. The injury mechanism, as well as the structural and physiological contributions of tissues in living human subjects are different than in cadaver legs, which requires further studies with subjects who have experienced various types of meniscal injuries. In particular, the frequency bands of interest introduced in the current work may change when the technology is translated to live subjects. Considering anatomical differences between male and female samples should be included in the study in the future to accommodate gender-related musculoskeletal variations. Future work will also involve an extended analytical model incorporating the effects of the soft tissues available in the human knee. The long-term goal of this study is to integrate the vibration stimuli technique into a wearable diagnostic device tuned at specific frequency ranges to be deployed for diagnosing various knee injuries in the field (e.g., military operations and sporting events), where the use of laboratory equipment is unfeasible. However, the stimulation needs to be provided by a miniature vibration actuator to implement as a wearable device. Insights gain in this study regarding the important frequency bands of vibration signals can help achieving a more compact stimulation mechanism. Beyond diagnostics, we envision a portable technology that can be used outside the clinical settings to monitor the joint condition longitudinally during the rehabilitation phase after the injury, with the goal of improving both the pace and efficacy of recovery.

REFERENCES

[1] G. Jacob, K. Shimomura, A. J. Krych, and N. Nakamura, "The meniscus tear: A review of stem cell therapies," *Cells*, vol. 9, no. 1, p. 92, Dec. 2019.

[2] K. A. Cullen, M. J. Hall, and A. Golosinskiy, "Ambulatory surgery in the United States, 2006," in *National Health Statistics Reports*, no. 11. Jan. 2009.

[3] H. B. Ellis, K. Wise, L. LaMont, L. Copley, and P. Wilson, "Prevalence of discoid meniscus during arthroscopy for isolated lateral meniscal pathology in the pediatric population," *J. Pediatric Orthopaedics*, vol. 37, no. 4, pp. 285–292, Jun. 2017.

[4] V. Couteaux *et al.*, "Automatic knee meniscus tear detection and orientation classification with mask-RCNN," *Diagnostic Interventional Imag.*, vol. 100, no. 4, pp. 235–242, Apr. 2019.

[5] D. Shakoor *et al.*, "Diagnosis of knee meniscal injuries by using three-dimensional MRI: A systematic review and meta-analysis of diagnostic performance," *Radiology*, vol. 290, no. 2, pp. 435–445, Feb. 2019.

[6] B. Song *et al.*, "3D-MRI combined with signal-to-noise ratio measurement can improve the diagnostic accuracy and sensitivity in evaluating meniscal healing status after meniscal repair," *Knee Surgery, Sports Traumatol., Arthroscopy*, vol. 27, no. 1, pp. 177–188, Jan. 2019.

[7] A. A. De Smet and R. Mukherjee, "Clinical, MRI, and arthroscopic findings associated with failure to diagnose a lateral meniscal tear on knee MRI," *Amer. J. Roentgenol.*, vol. 190, no. 1, pp. 22–26, Jan. 2008.

[8] J. N. Katz *et al.*, "Value of history, physical examination, and radiographic findings in the diagnosis of symptomatic meniscal tear among middle-aged subjects with knee pain," *Arthritis Care Res.*, vol. 69, no. 4, pp. 484–490, 2017.

[9] A. Speziali, G. Placella, M. M. Tei, A. Georgoulis, and G. Cerulli, "Diagnostic value of the clinical investigation in acute meniscal tears combined with anterior cruciate ligament injury using arthroscopic findings as golden standard," *Musculoskeletal Surg.*, vol. 100, no. 1, pp. 31–35, Apr. 2016.

[10] W. G. Kernohan, D. E. Beverland, G. F. McCoy, A. Hamilton, P. Watson, and R. Mollan, "Vibration arthrometry," *Acta Orthopaedica Scandinavica*, vol. 61, no. 1, pp. 70–79, Jan. 1990.

[11] H.-K. Jeong, M. B. Pouyan, D. C. Whittingslow, V. Ganti, and O. T. Inan, "Quantifying the effects of increasing mechanical stress on knee acoustical emissions using unsupervised graph mining," *IEEE Trans. Neural Syst. Rehabil. Eng.*, vol. 26, no. 3, pp. 594–601, Mar. 2018.

[12] C. N. Teague *et al.*, "Novel methods for sensing acoustical emissions from the knee for wearable joint health assessment," *IEEE Trans. Biomed. Eng.*, vol. 63, no. 8, pp. 1581–1590, Aug. 2016.

[13] C. N. Teague *et al.*, "A wearable, multimodal sensing system to monitor knee joint health," *IEEE Sensors J.*, vol. 20, no. 18, pp. 10323–10334, Sep. 2020, doi: 10.1109/JSEN.2020.2994552.

[14] D. C. Whittingslow, H.-K. Jeong, V. G. Ganti, N. J. Kirkpatrick, G. F. Kogler, and O. T. Inan, "Acoustic emissions as a non-invasive biomarker of the structural health of the knee," *Ann. Biomed. Eng.*, vol. 48, no. 1, pp. 225–235, Jan. 2020.

[15] H. K. Jeong, D. Whittingslow, and O. T. Inan, "B-value: A potential biomarker for assessing knee-joint health using acoustical emission sensing," *IEEE Sensors Lett.*, vol. 2, no. 4, pp. 1–4, Dec. 2018.

[16] R. A. Rusovici, D. B. Topping, S. E. S. Eriksson, and D. L. Lopez, "Experimental modal analysis of an *in-situ* clavicle," in *Proc. 41st Annu. Int. Conf. IEEE Eng. Med. Biol. Soc. (EMBC)*, Berlin, Germany, Jul. 2019, pp. 5352–5355.

[17] B. Zhou, K. J. Schaefbauer, A. M. Egan, E. M. Carmona Porquera, A. H. Limper, and X. Zhang, "An *ex vivo* technique for quantifying mouse lung injury using ultrasound surface wave elastography," *J. Biomech.*, vol. 98, Jan. 2020, Art. no. 109468.

[18] P. Avitabile, *Modal Testing: A Practitioner's Guide*. Hoboken, NJ, USA: Wiley, 2017.

[19] G.-Y. Li, Y. Zheng, Y.-X. Jiang, Z. Zhang, and Y. Cao, "Guided wave elastography of layered soft tissues," *Acta Biomater.*, vol. 84, pp. 293–304, Jan. 2019.

[20] D. Pereira, G. Haiat, J. Fernandes, and P. Belanger, "Effect of intra-cortical bone properties on the phase velocity and cut-off frequency of low-frequency guided wave modes (20–85 kHz)," *J. Acoust. Soc. Amer.*, vol. 145, no. 1, pp. 121–130, 2019.

[21] R. K. Lippmann, "The use of auscultatory percussion for the examination of fractures," *J. Bone Joint Surg.*, vol. 14, no. 1, pp. 118–126, 1932.

[22] L. Mattei, F. Di Puccio, and S. Marchetti, "Fracture healing monitoring by impact tests: Single case study of a fractured tibia with external fixator," *IEEE J. Translational Eng. Health Med.*, vol. 7, pp. 1–6, 2019.

[23] W. K. Chiu, B. S. Vien, M. Russ, and M. Fitzgerald, "Vibration-based healing assessment of an internally fixated femur," *J. Nondestruct. Eval., Diag. Prognostics Eng. Syst.*, vol. 2, no. 2, May 2019.

[24] A. S. Voloshin and J. Wosk, "Shock absorption of meniscectomized and painful knees: A comparative *in vivo* study," *J. Biomed. Eng.*, vol. 5, no. 2, pp. 157–161, Apr. 1983.

[25] A. Fok and H. P. Chew, "Stability of dental implants," in *Mathematical Models for Dental Materials Research*. Cham, Switzerland: Springer, 2020, pp. 55–64.

[26] N. Meredith, K. Books, B. Fribergs, T. Jemt, and L. Sennerby, "Resonance frequency measurements of implant stability *in viva*. A cross-sectional and longitudinal study of resonance frequency measurements on implants in the edentulous and partially dentate maxilla," *Clin. Oral Implants Res.*, vol. 8, no. 3, pp. 226–233, 1997.

[27] D. O'Sullivan, L. Sennerby, and N. Meredith, "Measurements comparing the initial stability of five designs of dental implants: A human cadaver study," *Clin. Implant Dentistry Rel. Res.*, vol. 2, no. 2, pp. 85–92, Apr. 2000.

[28] M. Lannocca, E. Varini, A. Cappello, L. Cristofolini, and E. Bialoblocka, "Intra-operative evaluation of cementless hip implant stability: A prototype device based on vibration analysis," *Med. Eng. Phys.*, vol. 29, no. 8, pp. 886–894, Oct. 2007.

[29] L. C. Pastrav, S. V. N. Jaecques, I. Jonkers, G. Van der Perre, and M. Mulier, "*In vivo* evaluation of a vibration analysis technique for the per-operative monitoring of the fixation of hip prostheses," *J. Orthopaedic Surg. Res.*, vol. 4, no. 1, p. 10, Dec. 2009.

[30] A. Arami, J.-R. Delaloye, H. Rouhani, B. M. Jolles, and K. Aminian, "Knee implant loosening detection: A vibration analysis investigation," *Ann. Biomed. Eng.*, vol. 46, no. 1, pp. 97–107, Jan. 2018.

[31] R. I. Ponder, M. Safaei, and S. R. Anton, "Validation of impedance-based structural health monitoring in a simulated biomedical implant system," in *Proc. Mech. Behav. Act. Mater.; Struct. Health Monit.; Bioinspired Smart Mater. Syst.; Energy Harvesting; Emerg. Technol.*, vol. 2. San Antonio, TX, USA, Sep. 2018, Art. no. V002T05A008.

[32] J. Pan, Z. Zhang, J. Wu, K. R. Ramakrishnan, and H. K. Singh, "A novel method of vibration modes selection for improving accuracy of frequency-based damage detection," *Compos. B, Eng.*, vol. 159, pp. 437–446, Feb. 2019.

[33] Z. Yang, X. Chen, J. Yu, R. Liu, Z. Liu, and Z. He, "A damage identification approach for plate structures based on frequency measurements," *Nondestruct. Test. Eval.*, vol. 28, no. 4, pp. 321–341, Dec. 2013.

[34] A. C. Altunişik, F. Y. Okur, S. Karaca, and V. Kahya, "Vibration-based damage detection in beam structures with multiple cracks: Modal curvature vs. modal flexibility methods," *Nondestruct. Test. Eval.*, vol. 34, no. 1, pp. 33–53, Jan. 2019.

[35] D. Montalvao, "A review of vibration-based structural health monitoring with special emphasis on composite materials," *Shock Vib. Dig.*, vol. 38, no. 4, pp. 295–324, Jul. 2006.

[36] R. Y. Liang, F. K. Choy, and J. Hu, "Detection of cracks in beam structures using measurements of natural frequencies," *J. Franklin Inst.*, vol. 328, no. 4, pp. 505–518, Jan. 1991.

[37] M. Boltezar, B. Strancar, and A. Kuhelj, "Identification of transverse crack location in flexural vibrations of free–free beams," *J. Sound Vib.*, vol. 211, no. 5, pp. 729–734, 1998.

[38] P. F. Rizos, N. Aspragathos, and A. D. Dimarogonas, "Identification of crack location and magnitude in a cantilever beam from the vibration modes," *J. Sound Vib.*, vol. 138, no. 3, pp. 381–388, May 1990.

[39] P. Guillaume, R. Pintelon, and J. Schoukens, "On the use of signals with a constant signal-to-noise ratio in the frequency domain," *IEEE Trans. Instrum. Meas.*, vol. 39, no. 6, pp. 835–842, Dec. 1990.

[40] V. Giurgiutiu and A. Zagrai, "Damage detection in thin plates and aerospace structures with the electro-mechanical impedance method," *Struct. Health Monit.: Int. J.*, vol. 4, no. 2, pp. 99–118, Jun. 2005.

[41] G. Marsaglia, W. W. Tsang, and J. Wang, "Evaluating Kolmogorov's distribution," *J. Stat. Softw.*, vol. 8, no. 18, pp. 1–4, 2003.

[42] M. E. Rice and G. T. Harris, "Comparing effect sizes in follow-up studies: ROC area, Cohen's d, and r," *Law Hum. Behav.*, vol. 29, no. 5, pp. 615–620, 2005.

[43] U. Meier, "A note on the power of Fisher's least significant difference procedure," *Pharmaceutical Statist.*, vol. 5, no. 4, pp. 253–263, 2006.

[44] P. Gerus *et al.*, "Subject-specific knee joint geometry improves predictions of medial tibiofemoral contact forces," *J. Biomech.*, vol. 46, no. 16, pp. 2778–2786, Nov. 2013.

[45] K. Markolf, J. Mensch, and H. Amstutz, "Stiffness and laxity of the knee–The contributions of the supporting structures. A quantitative *in vitro* study," *J. Bone Joint Surg.*, vol. 58, no. 5, pp. 583–594, Jul. 1976.

[46] S. S. Rao, *Vibration of Continuous Systems*. Hoboken, NJ, USA: Wiley, 2007.

[47] D. Goyal and B. S. Pabla, "The vibration monitoring methods and signal processing techniques for structural health monitoring: A review," *Arch. Comput. Methods Eng.*, vol. 23, no. 4, pp. 585–594, Dec. 2016.

[48] W. L. Li, "Free vibrations of beams with general boundary CONDITIONS," *J. Sound Vib.*, vol. 237, no. 4, pp. 709–725, Nov. 2000.

[49] J. W.-Z. Zu and R. P. S. Han, "Natural frequencies and normal modes of a spinning timoshenko beam with general boundary conditions," *J. Appl. Mech.*, vol. 59, no. 2S, pp. S197–S204, Jun. 1992.

[50] M. Eichinger, M. Schocke, C. Hoser, C. Fink, R. Mayr, and R. E. Rosenberger, "Changes in articular cartilage following arthroscopic partial medial meniscectomy," *Knee Surg., Sports Traumatol., Arthroscopy*, vol. 24, no. 5, pp. 1440–1447, May 2016.

[51] M. M. Petersen, C. Olsen, J. B. Lauritzen, B. Lund, and A. Hede, "Late changes in bone mineral density of the proximal tibia following total or partial medial meniscectomy: A randomized study," *J. Orthopaedic Res.*, vol. 14, no. 1, pp. 16–21, Jan. 1996.

[52] M. Safaei, N. B. Bolus, A. Erturk, and O. T. Inan, "Vibration characterization of the human knee joint in audible frequencies," *Sensors*, vol. 20, no. 15, p. 4138, Jul. 2020.